J Sol-Gel Sci Technol (2017) 81:138–146
DOI 10.1007/s10971-016-4090-4

ORIGINAL PAPER: SOL-GEL, HYBRIDS AND SOLUTION CHEMISTRIES

Carboxylic acid-functionalized porous silica particles by a co-condensation approach

Andrea Feinle[1] · Franz Leichtfried[1] · Sonja Straßer[1] · Nicola Hüsing[1]

Received: 3 March 2016 / Accepted: 21 May 2016 / Published online: 2 June 2016

Abstract Novel stable carboxylic acid derivatized alkoxy silanes are co-condensed with tetraethyl orthosilicate in the presence of a structure-directing agent in a direct "one-pot" synthesis to porous carboxy-modified silica particles. Special emphasis is given to the influence of an increasing amount of 5-(triethoxysilyl)pentanoic acid and sodium hydroxide on the morphology and porous structure of the co-condensation products. The simultaneous conversion of both silanes resulted in the formation of mesoporous, monodisperse spherical particles with diameters between 100 and 140 nm and specific surface areas up to 900 $m^2 g^{-1}$. Additionally, adsorption equilibrium studies were performed, in which the particles modified with carboxylic acid groups showed an increased adsorption rate toward methylene blue compared to pure silica materials.

Graphical Abstract

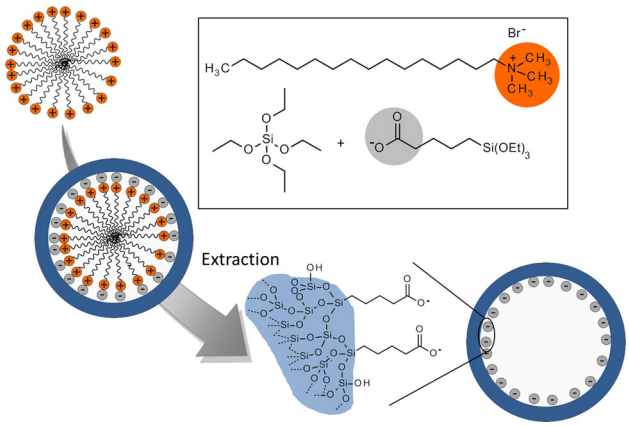

Keywords Carboxylic acid · Co-condensation · Silica · Sol–gel processing

1 Introduction

Hybrid mesoporous particles carrying functional organic groups have significantly broaden the application spectrum of pure silica materials, e.g., they can be used as adsorbents [1] or as active sites for biomolecule anchoring and polypeptide synthesis [2, 3]. Organofunctionalized silica materials are typically prepared via co-condensation reactions of two or more different silanes. Via this method, many different reactive groups can be introduced into the material [4–13]. However, if there is no silane available carrying the desired functionality, the reactive group must be generated in tedious multi step processes. Disadvantages and difficulties of this post-treatment are that (1) the

Electronic supplementary material The online version of this article (doi:10.1007/s10971-016-4090-4) contains supplementary material, which is available to authorized users.

✉ Andrea Feinle
andrea.feinle@sbg.ac.at

[1] Materials Chemistry, Paris Lodron University Salzburg, Hellbrunner Str. 34, 5020 Salzburg, Austria

functional groups have to be accessible for the reagents, (2) the reagents should not react with other functional groups or the silica surface, and (3) several synthetic steps are necessary resulting in cost- and time-intensive procedures.

Carboxylic acid-derivatized silica materials are mostly prepared by post-synthetic strategies comprising several steps, such as (1) hydrolysis of cyanides to carboxylic acid groups by adding concentrated sulfuric acid to the cyanide-modified silica particles [14–17], (2) hydrolysis of anhydride groups resulting in a material with a high density of carboxylic acid groups [18–20], or (3) hydrolysis of ester compounds [21]. Further synthetic approaches, possible applications and prospects of carboxylic group-functionalized ordered mesoporous silica materials are given in an excellent paper written by Han et al. [22].

Comparing co-condensation with post-synthetic reactions, the former is preferred in many cases. Reasons for this are that pore blocking, which is an inherent problem in subsequent modification reactions can be avoided and that the number of processing steps can be reduced to a minimum. However, only few papers are known in which carboxylic acid-derivatized silica materials are prepared via co-condensation of tetraalkoxysilanes with carboxylic acid-functionalized silanes [23–25]. This can be explained by the fact that only a few carboxylic acid-functionalized silanes are available [26, 27]. Markowitz et al. [23], for example, reported the possibility to synthesize SBA-15 mesoporous silicates with surface carboxylic acid groups by co-condensation of tetraethyl orthosilicate (TEOS) with a commercially available water-soluble sodium salt of the organosilane carboxyethylsilanetriol (CES). For carboxylic acid contents up to 5 wt%, the authors obtained mesoporous materials with a 2D hexagonal pore arrangement. However, copper binding studies revealed that the carboxy-modified materials showed no enhanced affinity for copper(II) ions, which make them unattractive as metal ion trapping agents. The possibility to use isolable carboxylic acid-functionalized trialkoxysilanes instead of CES was reported by Lin et al. [28]. For the co-condensation approach, the authors synthesized the carboxylic acid-modified, disulfide-containing organosilane, namely 2-[3-(trimethoxysilyl)-propyldisulfanyl]-propionic acid. A major advantage of the authors approach was the electrostatic matching effects between the anionic carboxylate-containing organoalkoxysilanes to the cationic headgroup of the CTAB surfactant. This supports on the one hand the formation of the silica network around the geometric arrangement of the surfactant molecule (resulting in silica materials with arranged mesopores) and on the other the preferred condensation of the carboxylic acid group at the silica–surfactant interface and therefore on the later pore surface. The synthesis, however, was not trivial and several reaction and purification steps were necessary to obtain the desired product.

In one of our recently published works, we demonstrated the possibility to synthesize stable carboxylic acid-derivatized alkoxysilanes via a convenient and straightforward one-pot hydrosilylation reaction of different unsaturated carboxylic acids with trialkoxysilanes in the presence of catalytic amounts of platinum(IV) dioxide [29]. We already reported the possibility to use these organosilanes as ligands for the complexation of europium(III)ions and the preparation of thin europium(III)-doped silica coatings [30]. In this paper, we report the suitability of 5-(triethoxysilyl)-pentanoic acid as a precursor molecule in the synthesis of carboxylic acid group containing siliceous materials using a co-condensation approach. Particular attention is given to the influence of an increasing amount of the carboxy-modified silane and sodium hydroxide on the morphology and structural properties of the materials.

2 Materials and methods

2.1 Materials

Tetraethyl orthosilicate (TEOS) and sodium hydroxide were purchased from Merck, cetyltrimethylammonium bromide (CTAB), methylene blue, and tetrahydrofuran (THF) from Sigma-Aldrich, and hydrochloric acid and ethanol (abs.) from VWR. All chemicals were used as purchased without further purification.

2.2 Synthesis of the carboxy-modified particles

5-(Triethoxysilyl)pentanoic acid was synthesized via hydrosilylation of pentenoic acid with triethoxysilane and platinum(IV) oxide as catalyst. The detailed synthesis is described elsewhere [29]. For the synthesis of carboxy-modified silica particles, 5-(triethoyxsilyl)pentanoic acid and TEOS were mixed and added to a mixture of preheated (80 °C) H_2O (26.7 mmol), CTAB (2.7 mmol), sodium hydroxide, and ethanol. For more information see Tables 1 and 2. After stirring for 2 h at 80 °C, the solid particles were separated from the solution by centrifugation and washed with ethanol three times. CTAB was extracted using a 1 mol solution of hydrochloric acid in tetrahydrofuran. To the resulting particles 100 mL of a 1 mol HCl solution in THF was added, and the mixture was stirred for 12 h under reflux conditions. Finally, the particles were separated from the HCl/THF solution and dried at 80 °C.

2.3 Adsorption equilibrium experiments

The basic dye methylene blue was investigated with respect to its adsorption behavior on carboxy-modified particles in comparison with pure silica materials.

Table 1 Molar amounts for the preparation of porous particles with different amounts of 5-(triethoxysilyl)pentanoic acid

	P0-7	P10-7	P20-7	P30-7	P35-7
H_2O	26.7 mol	26.7 mol	26.7 mol	26.7 mol	26.7 mol
CTAB	2.7 mmol	2.7 mmol	2.7 mmol	2.7 mmol	2.7 mmol
Ethanol	0 mmol	2.2 mmol	4.5 mmol	6.7 mmol	7.8 mmol
NaOH	7 mmol	7 mmol	7 mmol	7 mmol	7 mmol
TEOS	22.4 mmol	20.2 mmol	17.9 mmol	15.7 mmol	14.6 mmol
CS[a]	0 mmol	2.2 mmol	4.5 mmol	6.7 mmol	7.8 mmol

[a] CS: 5-(Triethoxysilyl)pentanoic acid

Table 2 Molar amounts for the preparation of porous particles modified with 10 mol% carboxylic acid groups and different amounts of sodium hydroxide

	P10-3.5	P10-7	P10-10.5	P10-21
H_2O	26.7 mol	26.7 mol	26.7 mol	26.7 mol
CTAB	2.7 mmol	2.7 mmol	2.7 mmol	2.7 mmol
Ethanol	2.2 mmol	2.2 mmol	2.2 mmol	2.2 mmol
NaOH	3.5 mmol	7.0 mmol	10.5 mmol	21.0 mmol
TEOS	20.2 mmol	20.2 mmol	20.2 mmol	20.2 mmol
CS[a]	2.2 mmol	2.2 mmol	2.2 mmol	2.2 mmol

[a] CS: 5-(Triethoxysilyl)pentanoic acid

In a typical experiment, 10 mg of the corresponding particles and 100 mL of the aqueous dye solution were stirred in a 180 mL polypropylene beaker at room temperature for 2 days. Prior to the UV/Vis measurements, the solid particles were removed from the dye solution by filtration over a polytetrafluoroethylene syringe filter with a membrane size of 100 nm. After filtration, the concentrations of the dye solutions were determined at the maximum absorbance wavelength of methylene blue (663 nm). To calculate the amount of the adsorbed dye, the following equation was used:

$$q_e = \frac{(C_0 - C_e) * V}{m} \quad (1)$$

with C_0 and C_e as the initial and the equilibrium concentrations of methylene blue (mmol L^{-1}), V as the volume of the dye solution (L), and m as the mass of the adsorbent (g).

2.4 Characterization

For nitrogen sorption measurements, all samples were degassed under vacuum at 100 °C for 12 h prior to analysis and measured on a Micromeritics ASAP 2420 at 77 K in the relative pressure range of $p/p_0 = 0.05$–0.99. The specific surface area was determined according to Brunauer et al. [31] by using the 5-point method in the relative pressure range of 0.05–0.30. The mesopore size distribution was calculated by the BJH method from the desorption branch [32]. Powder X-ray diffraction was carried out on a Bruker D8 Advance DaVinci device with Cu-K_α radiation ($\lambda = 0.1542$ nm). Scanning electron microscopy (SEM) was performed on a Zeiss ULTRA Plus operating at 1.5–5 kV accelerating voltage with an in-lens detector. IR-ATR spectra were recorded with a resolution of 4 cm^{-1} on a Bruker Vertex 70 spectrometer. UV/Vis measurements were performed on a PerkinElmer Lambda 750 device.

Simultaneous thermal analysis (STA) was performed on a STA 449 C Jupiter® (Netzsch) with a heating rate of 10 K min^{-1} in argon.

3 Results and discussion

Incorporation of organic groups in sol–gel materials by co-condensation is usually realized by a partial replacement of tetraalkoxysilanes by organofunctional trialkoxysilanes. This substitution has several consequences: first, the crosslinking density of the inorganic network is reduced, resulting in structural changes of the inorganic network [9, 13, 33–35]. Second, the organically modified trialkoxysilane exhibits a different hydrolysis and condensation behavior [36], which increases the risk of homo- instead of the desired heterocondensation [10]. Suitable organofunctional silanes should therefore show reaction rates in the same order as the corresponding tetraalkoxysilanes. Otherwise, an incorporation of organic groups in the silica network is hampered and only possible after other procedures, such as prehydrolysis of the slower reacting silane.

In this work, we investigate the possibility to introduce carboxylic acid groups into porous silica particles by applying the co-condensation approach of two different

silanes namely TEOS and 5-(triethoxysilyl)pentanoic acid under basic conditions. In the first part, special emphasis is given to structural changes of the silica network by an increasing amount of 5-(triethoxysilyl)pentanoic acid or sodium hydroxide as well as on the interaction of the growing silica matrix with the structure-directing agent CTAB. Due to the negative charged carboxylate group of 5-(triethoxysilyl)-pentanoic acid, the organosilane serves as a co-structure-directing agent (CSDA), providing strong electrostatic interactions with the cationic headgroups of the CTAB micelles. This bridging effect of the CSDA between the organic and the inorganic species favors their self-organization and the formation of a periodically arranged pore systems [25, 37].

In the second part, the successful incorporation of carboxylic acid groups in the silica matrix and their accessibility for basic dye molecules is discussed.

In summary, the following questions will be addressed in this work: (1) is it possible to incorporate highly reactive carboxylic acid groups by simple co-condensation sol–gel chemistry? (2) is there a limit regarding the amount of carboxylic acid groups that can be introduced? (3) does the co-condensation reaction in the presence of this silane result in a strong influence on the particle structure? and (4) can periodic pore structures by interaction with a suitable structure-directing agent, such as CTAB, be generated. Samples, described in this work are labeled as P_{x-y}, in which x indicates the molar percentage of 5-(triethoxysilyl)pentanoic acid related to the total molar amount of silicon centers of 22.4 mol and y indicates the millimolar amount of NaOH added to 22.4 mol silicon centers.

To study the influence of 5-(triethoxysilyl)pentanoic acid on the morphology and the structural properties of the particles, pure silica materials have been prepared under similar conditions and SEM images of all particles were taken (Fig. 1). For pure silica, the SEM images indicate a spherical shape of the particles with diameters of approximately 100 nm (Fig. 1a). Comparing this result with the SEM images of the carboxylic acid-modified particles, no influence of an increasing amount of 5-(triethoxysilyl)-pentanoic acid on the particle morphology can be observed. The particle diameter remains unaffected and varied independently from the carboxylic acid group content between 100 and 140 nm (Fig. 1b–e). However, a further increase in the carboxylic acid content was not possible. No particle formation was observed for approaches containing more than 35 mol% of the carboxy-modified silane.

Additionally, the influence of sodium hydroxide on the morphology of carboxylic acid-modified silica particles was investigated. For this, particles containing the theoretical amount of 10 mol% carboxylic acid groups were prepared with different amounts of sodium hydroxide. In contrast to the previously prepared samples containing different amounts of carboxylic acid groups, the amount of sodium hydroxide significantly affects the pH value of the sol. It rises from pH 6.9 (for the sample P10-3.5) over pH 8.9 (P10-7) and 10.4 (P10-10.5) to pH 10.7 (P10-21). Figure 1f–h demonstrates the influence of the increasing pH value on the morphology of the particles: with increasing pH, the spherical shape is completely lost and larger bean-like particles are formed.

The nitrogen adsorption–desorption isotherms and the pore size distributions that were calculated from the adsorption branch of the isotherm with the BJH method are shown in Fig. 2. For the particles prepared with different amounts of 5-(triethoxysilyl)pentanoic acid, all isotherms show a sharp increase in the adsorbed volume between relative pressures of 0.2 and 0.5, indicating the presence of small pores. In the case of pure silica particles, the isotherms show a hysteresis loop whose intensity decreases and finally disappears with increasing carboxylic acid content. This indicates a broader pore size distribution and a decrease in the pore diameters. Both can be confirmed by BJH calculations (Fig. 2 bottom). With increasing carboxylic acid content, the width of the pore size distribution significantly increases and the maximum is shifted toward smaller pore diameters. This can be explained by the fact that an increasing inclusion of the relatively large carboxylic acid groups causes steric repulsions at the interface between the growing hybrid network and the positively charged CTAB micelles. These steric repulsions force the curvature of the micelle assembly to increase, whereby the diameter is decreased [38, 39].

For the particles prepared by varying the proportion of sodium hydroxide while keeping the amount of carboxylic acid groups constant, a similar trend can be observed. Both graphs on the right side of Fig. 2 illustrate the high dependency of the porosity on the amount of added sodium hydroxide. The samples P10-7 and P10-10.5 show a narrow pore size distribution, whereas for the samples prepared with lower or higher amounts of sodium hydroxide no or only a very broad pore size distribution was obtained. From this, it can be concluded that only with a defined amount of sodium hydroxide, a well-pronounced pore system can be obtained and that therefore the amount of sodium hydroxide in the sol must be well adjusted. This strong dependence of the pore structure on the amount of sodium hydroxide or the alkalinity of the system has already been reported by Che et al. [25]. The authors addressed the problem that under strong alkaline conditions CES is highly hydrated and therefore exhibit only weak interactions with the cationic headgroup of the surfactant. As a result, the mesocages composed of CES and the surfactant micelles have a positive charge, resulting in highly repulsive forces. In contrast, under low alkaline conditions CES

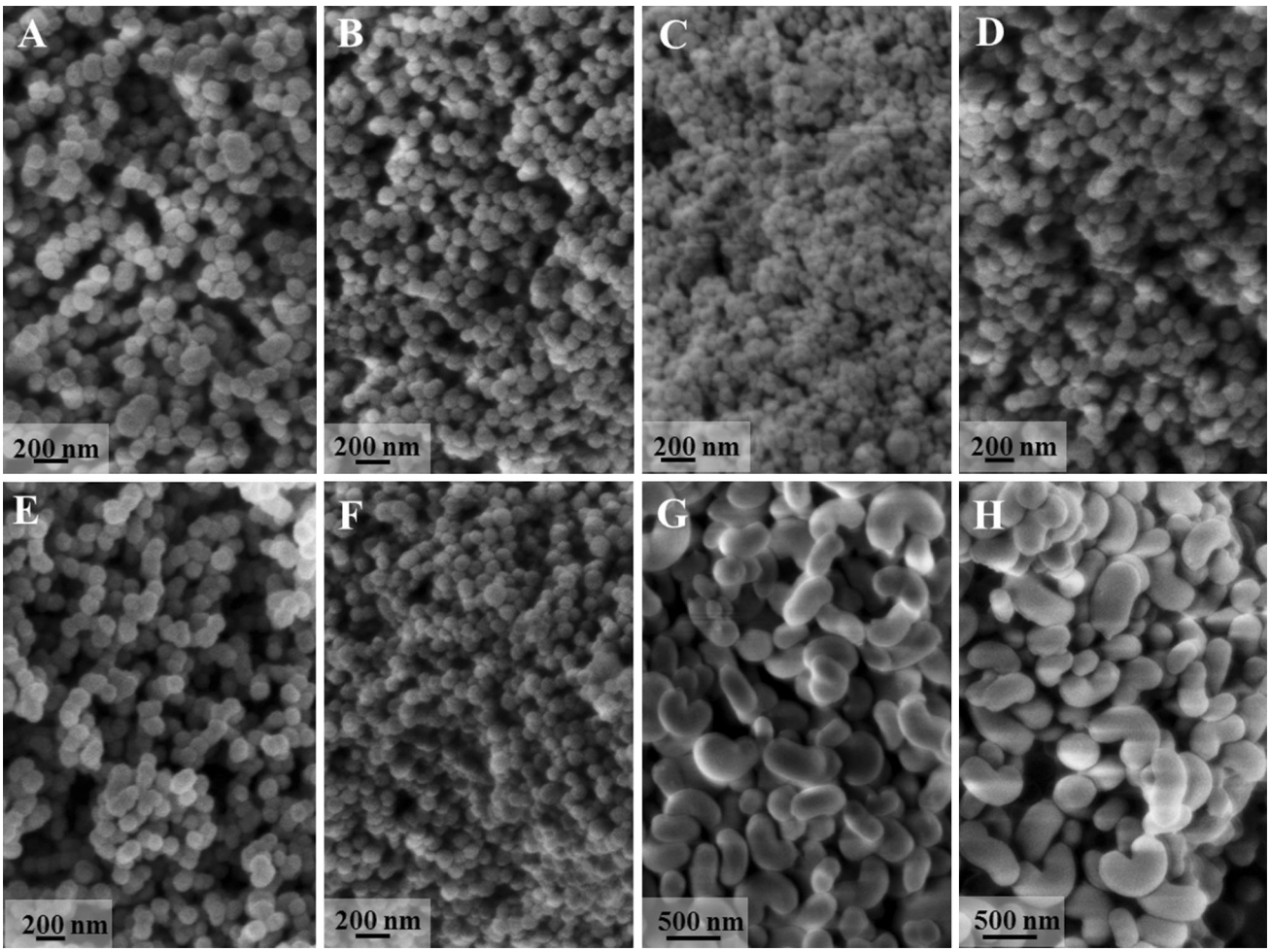

Fig. 1 SEM images of silica particles modified with various amounts of carboxylic acid groups and sodium hydroxide amounts. **a** P0-7, **b** P10-7, **c** P20-7, **d** P30-7, **e** P35-7, **f** P10-3.5, **g** P10-10.5, **h** P10-21

is less hydrated and therefore has strong electrostatic interactions with the surfactant micelles. As a consequence, the positive charge density and the repulsive forces of the mesocages are low and a regular arrangement of the micelles is enhanced.

The calculated specific surface areas (SSA) and the pore sizes of all prepared particles are summarized in Fig. 3. All samples exhibit high specific surface areas up to 1040 $m^2\ g^{-1}$. Only high amounts of carboxylic acid groups or sodium hydroxide lead to slightly lower specific surface areas of 570 or 770 $m^2\ g^{-1}$, respectively. This is due to a loss in the mesopore volume.

The pore sizes initially rise from 2.6 nm for the pure silica particles to 3.0 nm for the carboxylic acid-modified particles and subsequently show a clear tendency to smaller pores with increasing carboxylic acid or sodium hydroxide content. For the sample P10-21, no clear pore diameter could be calculated due to the very broad pore size distribution.

To investigate the spatial arrangement of the pores, all samples were characterized via X-ray diffraction. In Figs. 4 and 5, the diffraction patterns as well as the structural parameters of the carboxy-modified particles after extraction of the surfactant are shown.

The pure silica particles as well as the particles modified with 10 mol% carboxylic acid groups show a long-range-ordered 2D hexagonal arrangement of the mesopores with three well-pronounced scattering peaks at 2.13°, 3.69°, and 4.26° 2θ. The d-spacing ration of $1:\sqrt{3}:2$ can be indexed to the (10), (11), and (20) Bragg reflections from which the respective lattice d-spacings d_{10}, d_{11}, and d_{20} can be calculated. For the particles modified with higher amounts of carboxylic acid groups, the (10) peak is strongly broadened and the (11) and (20) peaks are no longer detectable. This shows that a higher number of carboxylic acid groups results in a less pronounced hexagonal arrangement of the mesopores within the organic–inorganic matrix. This negative effect of organofunctional trialkoxysilanes on the

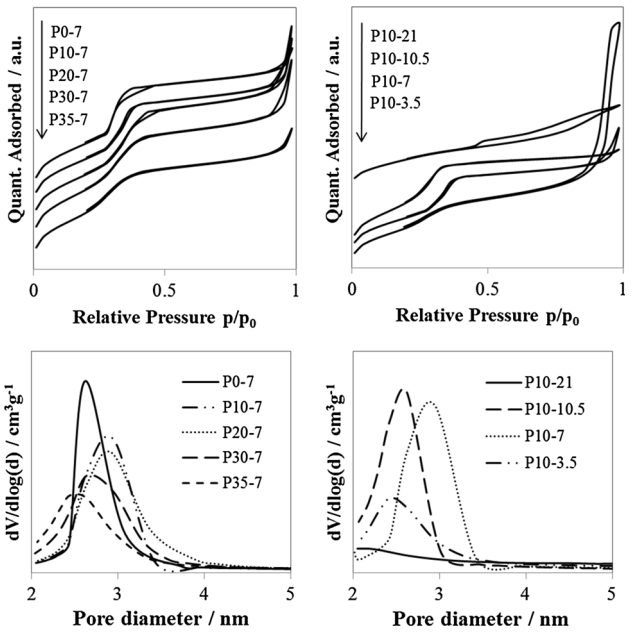

Fig. 2 Adsorption/desoprtion isotherms and pore size distribution of the samples prepared with different amounts of 5-(triethoxysilyl)pentanoic acid (*left*) and sodium hydroxide (*right*)

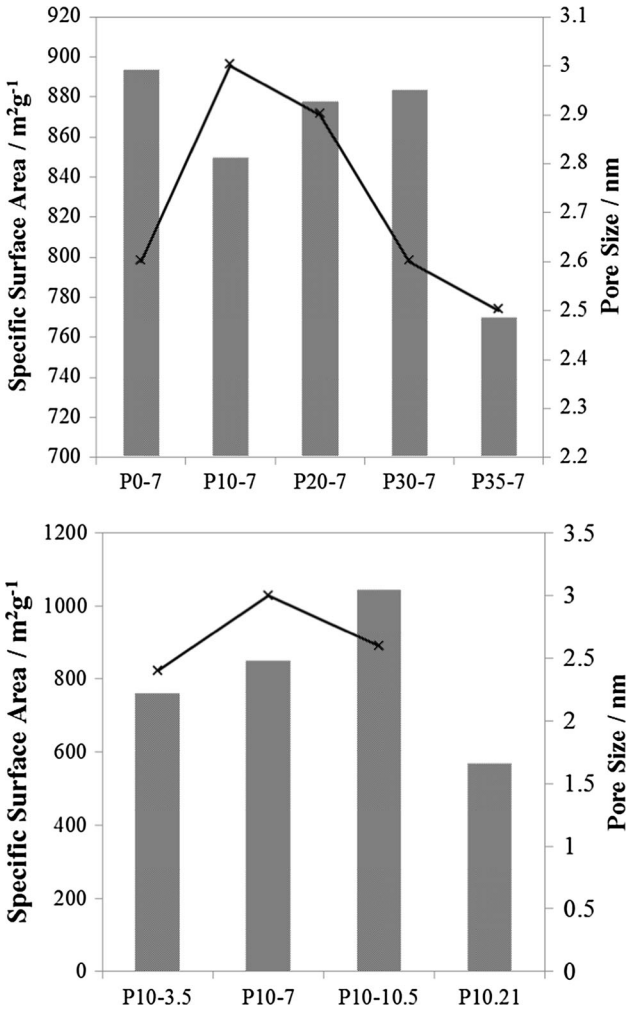

Fig. 3 Specific surface area and pore sizes of particles prepared with different amounts of 5-(triethoxysilyl)pentanoic acid (*top*) or sodium hydroxide (*bottom*). Lines present the pore sizes in nm; *bars* stand for the specific surface area in $m^2\ g^{-1}$; *lines* are drawn for clarity

pore structure has already been described by Richer et al. [39]. The authors explained this influence with the increased lyophilic interactions between organosilanes and the hydrophobic core of micelles. This leads to an opening of the micelle structure and causes a deeper penetration of TEOS into the micelles. Consequently, the micelle organization is perturbed and more disordered domains are formed.

All calculated parameters for the 2D hexagonal lattice are presented in Fig. 4 (bottom). For the carboxylic acid-modified particles, a slight peak shift toward smaller q- and therefore larger lattice spacings (d_{10}) as well as lattice constants (a) is observed. Additionally, the thicknesses of the walls in the materials were estimated. Due to the increasing lattice spacings and the decreasing pore sizes, thicker organically modified silica walls are obtained. The thickness increases from 2.1 nm for the sample modified with 10 mol% of carboxylic acid groups (P10-7) to 3.0 nm for the sample prepared with 30 mol% carboxylic acid groups (P30-7).

For the particles prepared with different amounts of sodium hydroxide, the most pronounced 2D hexagonal arrangement of the mesopores can be obtained for a sodium hydroxide content of 10.5 mmol (P10-10.5). Compared to the diffraction patterns of the other samples with lower or higher sodium hydroxide contents, it can clearly be seen that the amount of NaOH should be between 7 and 10.5 mmol. Out of this range, instead of sharp reflections indicating a long-range-ordered pore arrangement, the scattering curves show a weak short-range-order peak. Particularly, the addition of high amounts of sodium hydroxide leads to a complete loss of the structural ordering.

Figure 6 shows the IR-ATR spectra of the nanoparticles prepared with different amounts of carboxylic acid-modified silanes. The most intense peaks can be identified as follows: (1) $\sim$455 cm^{-1} (Si–O rocking vibration), (2) $\sim$804 cm^{-1} (Si–O bending vibration), (3) $\sim$968 cm^{-1} (Si–O(H–H_2O) bending vibration), and (4) 1072 (asymmetric stretching vibration of Si–O–Si). The vibration band at $\sim$1720 cm^{-1} corresponds to the CO vibration of the carboxylic acid group [40]. With increasing amount of organofunctional silane, hence carboxylic acid group, an increase in the band intensity can be observed. This clearly proves the presence of carboxylic acid groups in the silica

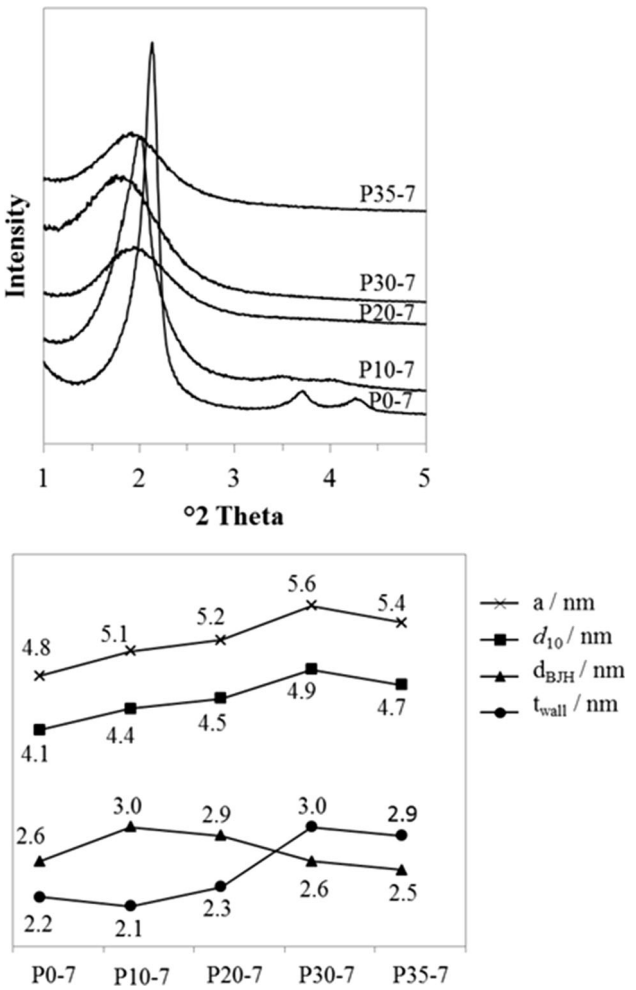

Fig. 4 X-ray diffraction patterns and structural parameters such as d_{10}, a, d_{ads}, t_{wall}, of the particles prepared with different amounts of 5-(triethoxysilyl)pentanoic acid. *Curves* are shifted vertically and *lines* are drawn for clarity

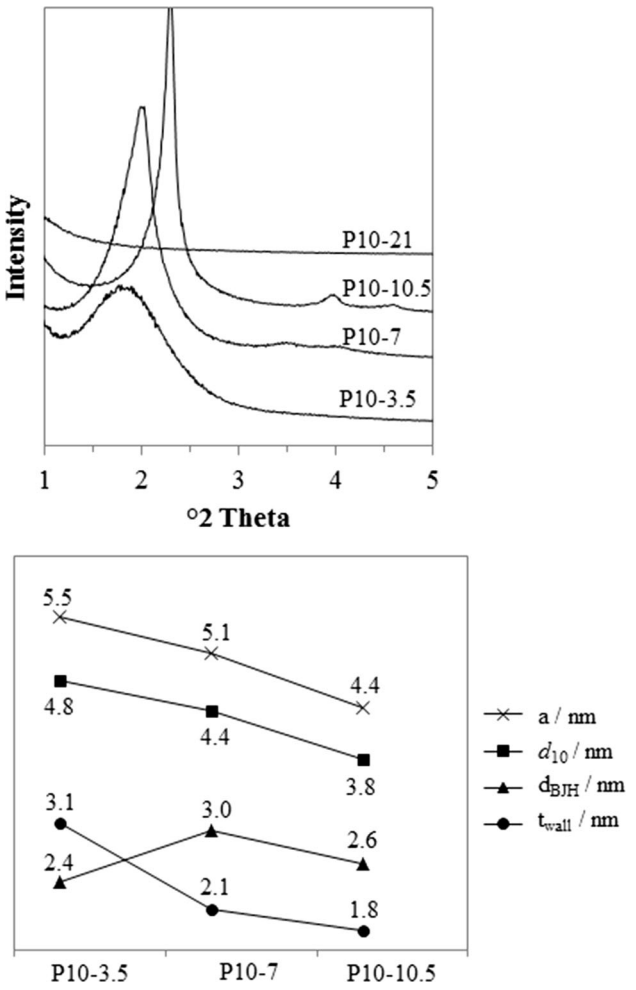

Fig. 5 X-ray diffraction patterns and structural parameters such as d_{10}, a, d_{ads}, and t_{wall}, of the particles prepared with different amounts of sodium hydroxide. *Curves* are shifted vertically and *lines* are drawn for clarity

matrix, and the formation of ester compounds can be excluded.

To compare the theoretical amount of the carboxylic acid groups with the actual amount of the carboxylic acid groups that are incorporated in the particles, STA measurements were performed (Fig. S1). However, the data show that a complete removal of the surfactant from the pores was not possible. For this reason, precise quantitative evaluations are not possible.

Carboxylic acid group-functionalized materials are often used as adsorbent materials due to the affinity and high binding capacity, e.g., toward basic dye molecules. Under neutral or basic conditions, all carboxylic acid groups are deprotonated and present in the form of negatively charged carboxy groups. Particularly, these negatively charged moieties are very suitable as binding sites for the adsorption of, e.g., methylene blue, onto the particles through electrostatic interactions. This effect has already been

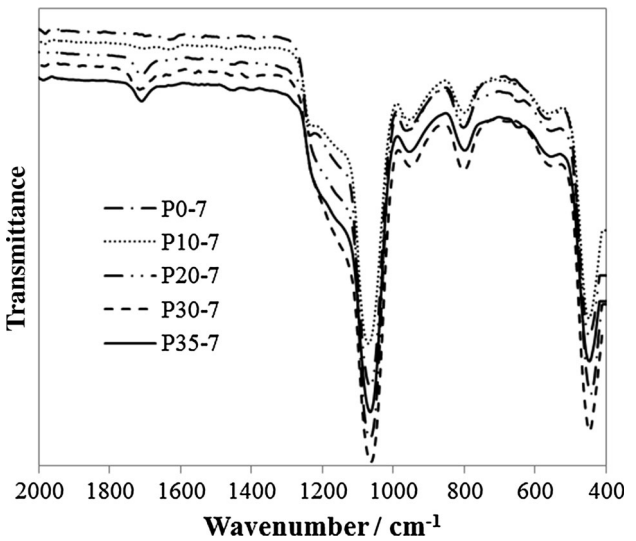

Fig. 6 IR-ATR spectra of the particles, prepared with different amounts of 5-(triethoxysilyl)pentanoic acid

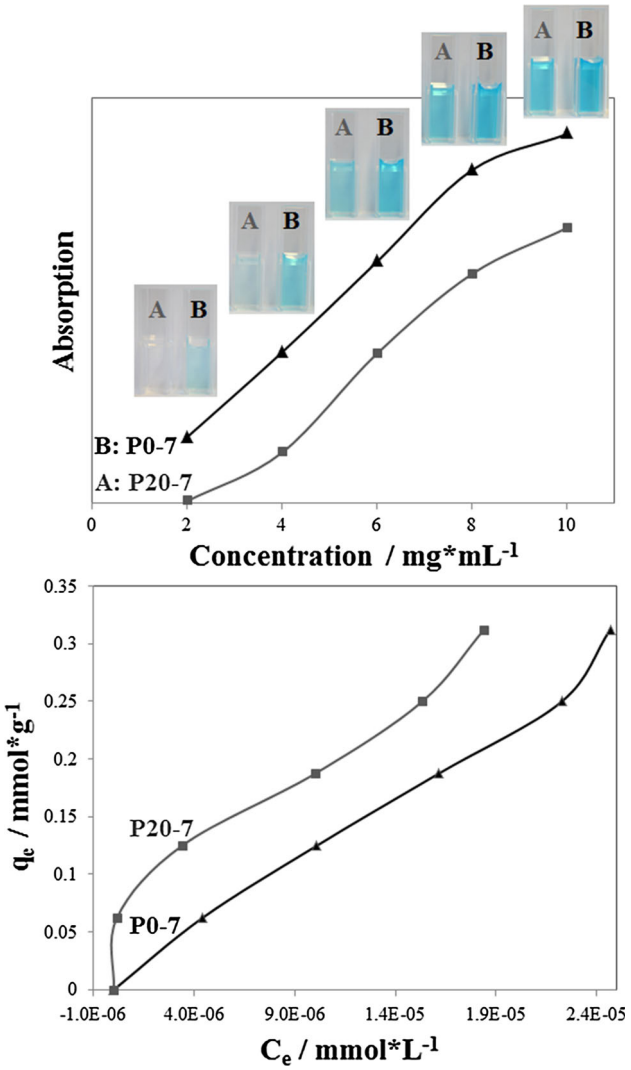

Fig. 7 *Top* UV/Vis signal intensities measured at 663 nm for the dye solutions after the adsorption experiment. The *insets* show pictures of the solutions after separation from the particles. *Bottom* Equilibrium adsorption isotherms of methylene blue onto the porous particles

reported by Li et al. [18] who further described the dependency of the pore size and the specific surface area on the adsorption capacity. In our adsorption experiments, we compared pure silica particles with particles, modified with 20 wt% carboxylic acid groups. Since both samples (P0-7 and P20-7) have almost the same pore size and specific surface area, the carboxylate groups should be responsible for the different adsorption behavior of the two samples. Figure 7 shows the adsorption behavior of both set of particles toward aqueous methylene blue solutions with concentrations between 2 and 10 mg mL^{-1} as well as the adsorption isotherms of methylene blue on the porous particles. In both cases, the adsorption capacities are higher than those of conventional adsorbents, such as glass fibers, pyrophyllite or activated petroleum [41–43] and comparable to the values reported for similar silica or carboxy-modified silica particles [14, 18]. From both graphs, it is obvious that during the same time interval of 2 days, more dye is adsorbed on the surface of carboxy-modified particles than on pure silica materials. This different adsorption behavior is even visible by eye. Photographs of the individual samples after separation of the particles are shown in the insets of Fig. 7. The images show that an aqueous methylene blue solution with a concentration of 2 mg mL^{-1} was completely discolored after stirring with carboxy-modified silica particles for 2 days. In contrast, pure silica particles, even comprising mesopores, could not completely adsorb the dye and a weak blue colored solution remained. This trend is also continued for the other concentrations of methylene blue in water illustrating that carboxy-modified particles have a larger tendency to adsorb basic dyes than pure silica materials. In this respect, carboxy-modified particles are highly interesting materials for the development of efficient adsorbents for the removal of pollutants, e.g., heavy metals from waste water. However, further adsorption experiments are necessary.

4 Conclusions

A simple, straightforward one pot co-condensation approach has been presented for 100 to 140 nm-sized spherical carboxy-modified particles. Quantification of the carboxylic acid groups was not possible, but IR-ATR measurements clearly prove the incorporation of the functional groups in the silica network. High specific surface areas were obtained and the adsorption behavior of the carboxy-modified particles toward methylene blue was improved compared to pure silica materials. This illustrates the suitability of the particle as adsorbent materials and further studies on this issue will follow.

Acknowledgments Open access funding provided by Paris Lodron University of Salzburg. The authors thank the Deutsche Forschungsgemeinschaft (HU 1427/4-1) and the University of Salzburg for financial support with the framework of Allergy-Cancer-BioNano Research Center. G. Tippelt and M. Suljic are acknowledged for the X-ray diffraction patterns and the nitrogen sorption measurements.

References

1. Bruzzoniti MC, Prelle A, Sarzanini C, Onida B, Fiorilli S, Garrone E (2007) J Sep Sci 30:2414–2420
2. Yu Y, Chen B, Qi W, Li X, Shin Y, Lei C, Liu J (2012) Microporous Mesoporous Mater 153:166–170
3. Colilla M, Izquierdo-Barba I, Sánchez-Salcedo S, Fierro JL, Hueso JL, Ma Vallet-Regí (2010) Chem Mater 22:6459–6466
4. Hüsing N, Schwertfeger F, Tappert W, Schubert U (1995) J Non-Cryst Solids 186:37–43
5. Hüsing N, Brandhuber D, Kaiser P (2006) J Sol-Gel Sci Technol 40:131–139
6. Keppeler M, Hüsing N (2011) New J Chem 35:681–690
7. Keppeler M, Holzbock J, Akbarzadeh J, Peterlik H, Hüsing N (2011) Beilstein J. Nanotechnol. 2:486–498
8. Burkett SL, Sims SD, Mann S (1996) Chem Commun 1367–1368
9. Huh S, Wiench JW, Yoo J-C, Pruski M, Lin VS-Y (2003) Chem Mater 15:4247–4256
10. Burleigh MC, Markowitz MA, Spector MS, Gaber BP (2001) J Phys Chem B 105:9935–9942
11. Sujandi Park S, Han D, Han S, Jin M, Ohsuna T (2006) Chem Commun 4131–4133
12. Yokoi T, Yoshitake H, Tatsumi T (2004) J Mater Chem 14:951–957
13. Sadasivan S, Khushalani D, Mann S (2003) J Mater Chem 13:1023–1029
14. Ho KY, McKay G, Yeung KL (2003) Langmuir 19:3019–3024
15. Yang C-M, Zibrowius B, Schüth F (2003) Chem Commun 1772–1773
16. Liu N, Assink RA, Brinker CJ (2003) Chem Commun 370–371
17. Fiorilli S, Onida B, Bonelli B, Garrone E (2005) J Phys Chem B 109:16725–16729
18. Yan Z, Tao S, Yin J, Li G (2006) J Mater Chem 16:2347–2353
19. Chang B, Guo J, Liu C, Qian J, Yang W (2010) J Mater Chem 20:9941–9947
20. Fu X, Chen X, Wang J, Liu J (2011) Microporous Mesoporous Mater 139:8–15
21. Yang Q, Wang S, Fan P, Wang L, Di Y, Lin K, Xiao F-S (2005) Chem Mater 17:5999–6003
22. Han L, Terasaki O, Che S (2011) J Mater Chem 21:11033–11039
23. Markowitz MA, Klaehn J, Hendel RA, Qadriq SB, Golledge SL, Castner DG, Gaber BP (2000) J Phys Chem B 104:10820–10826
24. Han L, Sakamoto Y, Terasaki O, Li Y, Che S (2007) J Mater Chem 17:1216–1221
25. Gao C, Che S (2010) Adv Funct Mater 20:2750–2768
26. Kayan A, Hoebbel D, Schmidt H (2005) J Appl Polym Sci 95:790–796
27. Silva PR, Almeida VO, Machado GB, Benvenutti EV, Costa TM, Gallas MR (2011) Langmuir 28:1447–1452
28. Radu DR, Lai CY, Huang J, Shu X, Lin VSY (2005) Chem Commun 1264–1266
29. Feinle A, Flaig S, Puchberger M, Schubert U, Hüsing N (2015) Chem Commun 2339–2341
30. Feinle A, Lavoie-Cardinal F, Akbarzadeh J, Peterlik H, Adlung M, Wickleder C, Hüsing N (2012) Chem Mater 24:3674–3683
31. Brunauer S, Emmett PH, Teller E (1938) J Am Chem Soc 60:309–319
32. Barrett EP, Joyner LG, Halenda PP (1951) J Am Chem Soc 73:373–380
33. Hodgkins RP, Garcia-Bennett AE, Wright PA (2005) Microporous Mesoporous Mater 79:241–252
34. Möller K, Kobler J, Bein T (2007) J Mater Chem 17:624–631
35. C-m Yang, Wang Y, Zibrowius B, Schüth F (2004) Phys Chem Chem Phys 6:2461–2467
36. Torma V, Peterlik H, Bauer U, Rupp W, Hüsing N, Bernstorff S, Steinhart M, Goerigk G, Schubert U (2005) Chem Mater 17:3146–3153
37. Che S, Garcia-Bennett AE, Yokoi T, Sakamoto K, Kunieda H, Terasaki O, Tatsumi T (2003) Nat Mater 2:801–805
38. Mercier L, Pinnavaia TJ (2000) Chem Mater 12:188–196
39. Richer R, Mercier L (1998) Chem Commun 1775–1777
40. Fiorilli S, Camarota B, Garrone E, Onida B (2011) Phys Chem Chem Phys 13:1201–1209
41. Shawwa AR, Smith DW, Sego DC (2001) Water Res 35:745–749
42. Chakrabarti S, Dutta BK (2005) J Colloid Interface Sci 286:807–811
43. Gücek A, Şener S, Bilgen S, Mazmancı MA (2005) J Colloid Interface Sci 286:53–60